Supplementary Material

Supplemental Items:

<u>Supplemental Figures</u>

Supplemental Figure S15. miRNA-27a-AT negatively regulates miR-27a expression and affects cell proliferation.

Supplemental Figure S16. Examples of miRNA-ATs in imprinted loci.

Supplemental Tables

Supplemental Table S1. High-throughput sequencing data summary.

Supplemental Table S2. A-to-I RNA editing sites in miRNA-ATs.

Supplemental Table S3. Sanger sequencing verification of selected T-to-C sites.

Supplemental Table S4. miRNA-ATs that are overlapped with FANTOM5 5'complete transcripts.

Supplemental Table S5. The genic positions of miRNA-ATs.

Supplemental Table S6. Primer sequences and gene sequences synthesized in this study.

Supplemental Table S7. gRNA sequences used for dCas9-based transcriptional regulation.

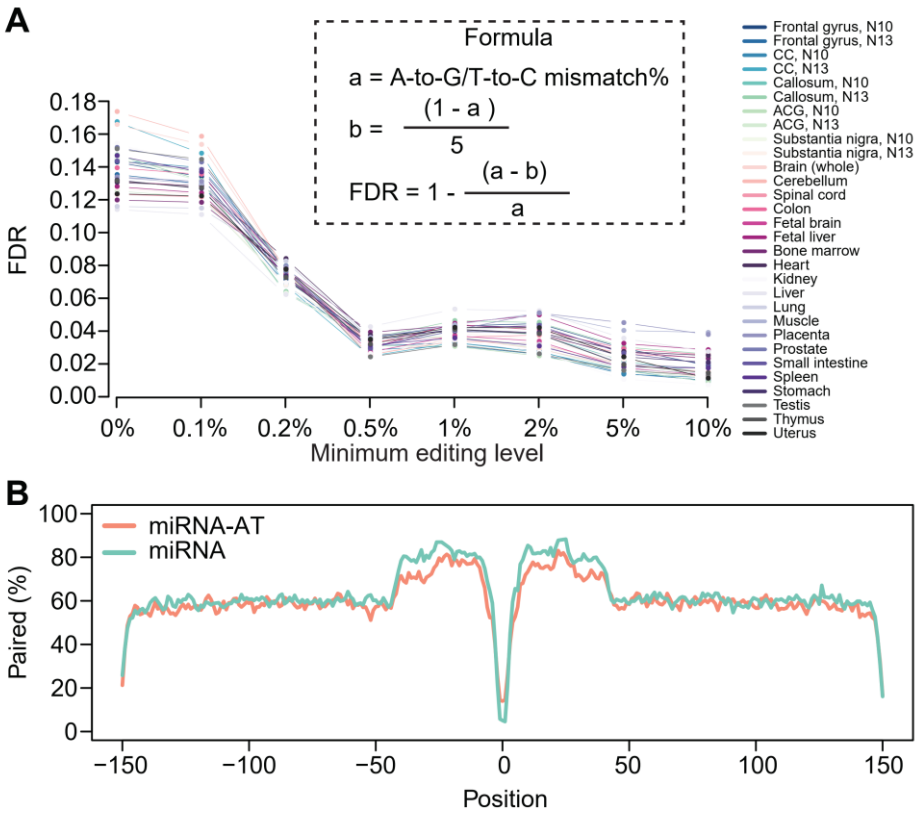

Supplemental Figure S1. Identification of RNA editing sites in miRNA-ATs.

(**A**) Relationship between the FDR of A-to-I RNA editing site identification and minimum editing levels.

(B) Metaprofiles of the secondary structure of the pre-miRNAs or the regions of miRNA-ATs that are opposite to the pre-miRNAs and the flanking regions. Sequences were folded with the RNAfold tool in ViennaRNA Package. Position 0 of a miRNA/miRNA-AT is defined as the central position of the loop region of a pre-miRNA. The negative value, the distance between an upstream position and the central position; the positive value, the distance between a downstream position and the central position. The percentage of paired bases at each position was calculated.

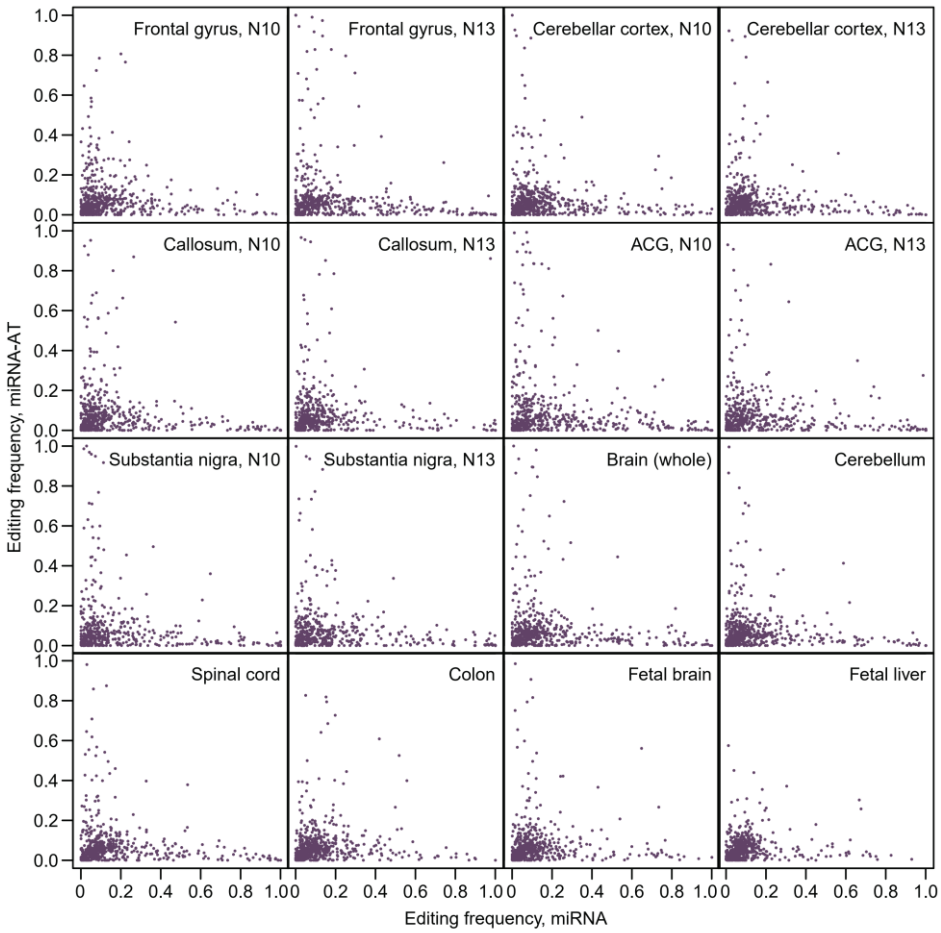

Supplemental Figure S2. Comparison of editing frequency between sense-antisense miRNA pairs.

For a given miRNA locus, editing frequency of the miRNA was defined as the number of reads with at least one G in the editing positions divided by the total number of reads covered in this locus. Similarly, editing frequency of the miRNA-AT was defined as the number of reads with at least one C in the antisense editing positions divided by the total number of reads covered in this locus. Only miRNA loci with coverage ≥ 30 in miR-mmPCR-seq data were used in this analysis.

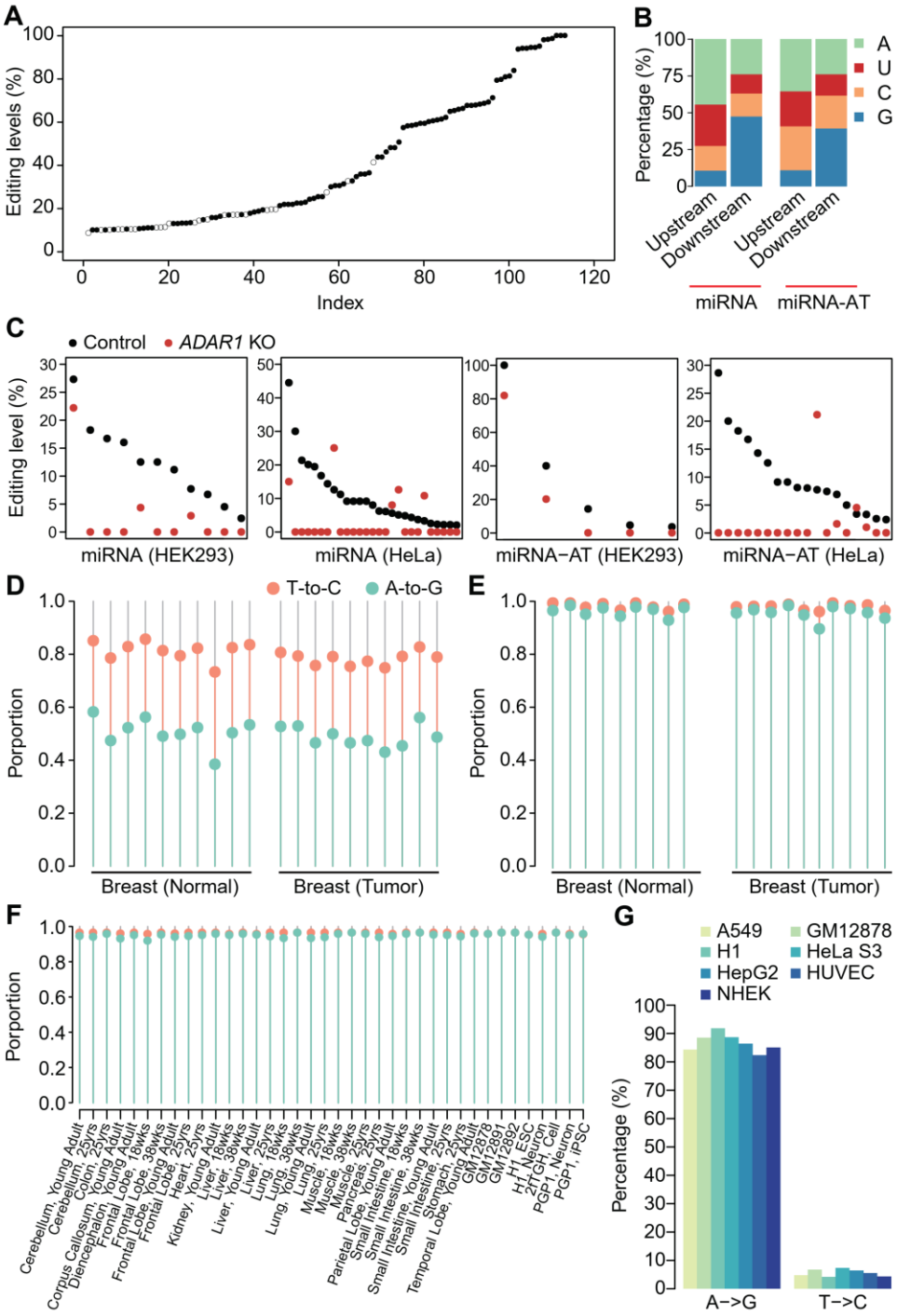

Supplemental Figure S3. Validation of editing sites in miRNA-ATs.

(A) Sanger validation of A-to-I RNA editing sites in miRNA-ATs. Solid circle, validated; hollow circle, non-validated. Sites were sorted by editing levels measured from miR-mmPCR-seq.

(**B**) Nucleotide composition in positions immediately upstream and downstream of the edited sites in miRNAs and miRNA-ATs. The top 500 editing sites with high editing levels were selected for analysis.

(**C**) Comparison of editing level of sites identified in miRNAs and miRNA-ATs between wild-type and *ADAR1* knockout HEK293 and HeLa cells. For HEK293 cells, stranded mRNA-seq libraries constructed in this study were analyzed. For HeLa cells, rRNA-depleted stranded RNA-seq data from a previous study were analyzed (Pfaller et al. 2018). A-to-I editing sites with coverage ≥ 5 in both samples and with editing level > 0.02 in wild-type cells were used in this analysis.

(D-E) The percentage of A-to-G and T-to-C mismatch types among the all 12 mismatch types in miRNA loci (**D**) or mRNA loci (**E**) in human breast normal and tumor samples. Sites with editing level ≥2% were used for analysis. The miRNA editing and mRNA editing profiles of 10 pairs of matched breast normal and tumor samples, which were used to identify tumor relevant editing events (Chen et al. unpublished data), were used for analysis.

(F) The percentage of A-to-G and T-to-C mismatch types among the all 12 mismatch types in mRNA editing loci in multiple types of human tissues and cells. The mmPCR-seq data was obtained from our previous study (SRP039090). The reads from replicates of the same tissue/cell type were merged for analysis. Sites with editing level ≥2% were used for analysis.

(G) The percentage of A-to-G and T-to-C mismatch types among the all 12 mismatch types in mRNA 3'UTR *Alu* regions without antisense transcription. Stranded mRNA-seq data of 7 cell lines were obtained from the ENCODE Project. Sites with editing level ≥2% were used for analysis.

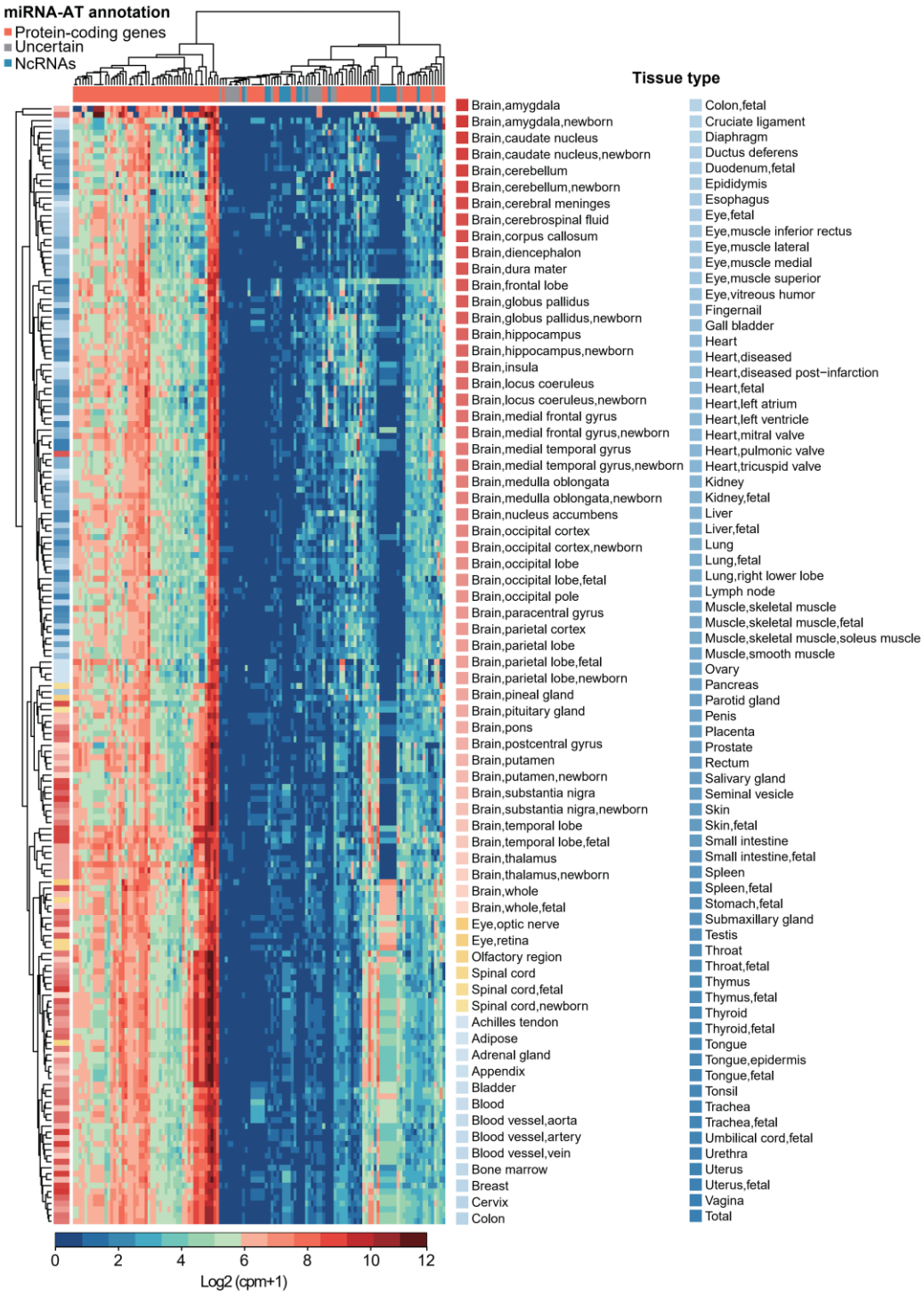

Supplemental Figure S4. The expression dynamics of miRNA-ATs profiled using FANTOM5 CAGE data.

The dendrogram was drawn based on the distance metric computed by all miRNA-ATs. cpm, counts per million. The FANTOM5 annotation was used to define the pri-miRNAs and miRNA-ATs. The FANTOM5 CAGE data was used to quantify their expressions.

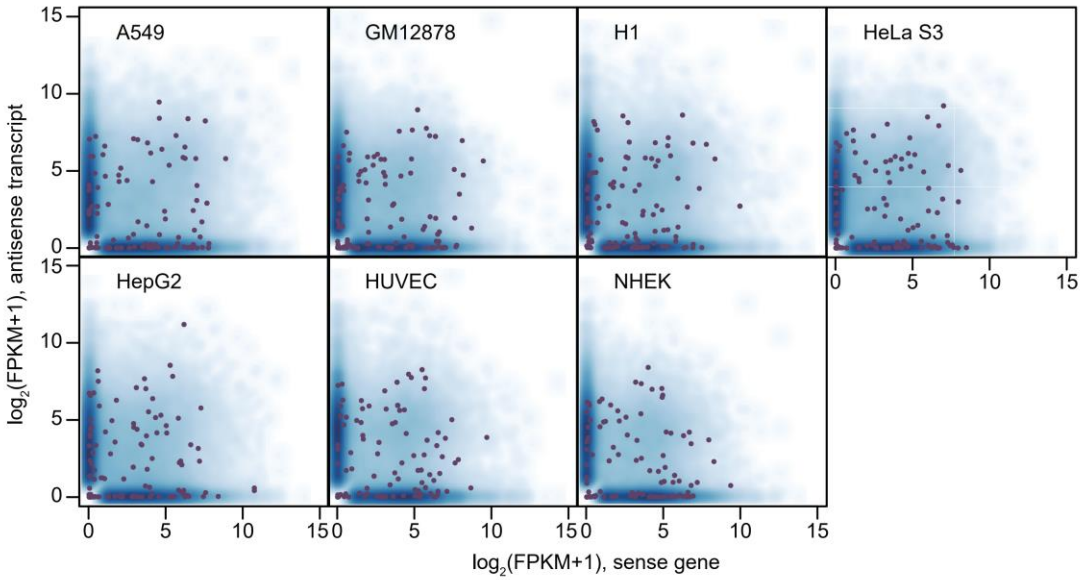

Supplemental Figure S5. Comparison of expression levels between sense-antisense miRNA pairs.

Stranded mRNA-seq data of nuclear RNA from 7 cell lines of the ENCODE Project were analyzed. Each dot represents a sense-antisense miRNA pair. Protein-coding genes and their paired antisense transcripts were plotted as background (blue shade).

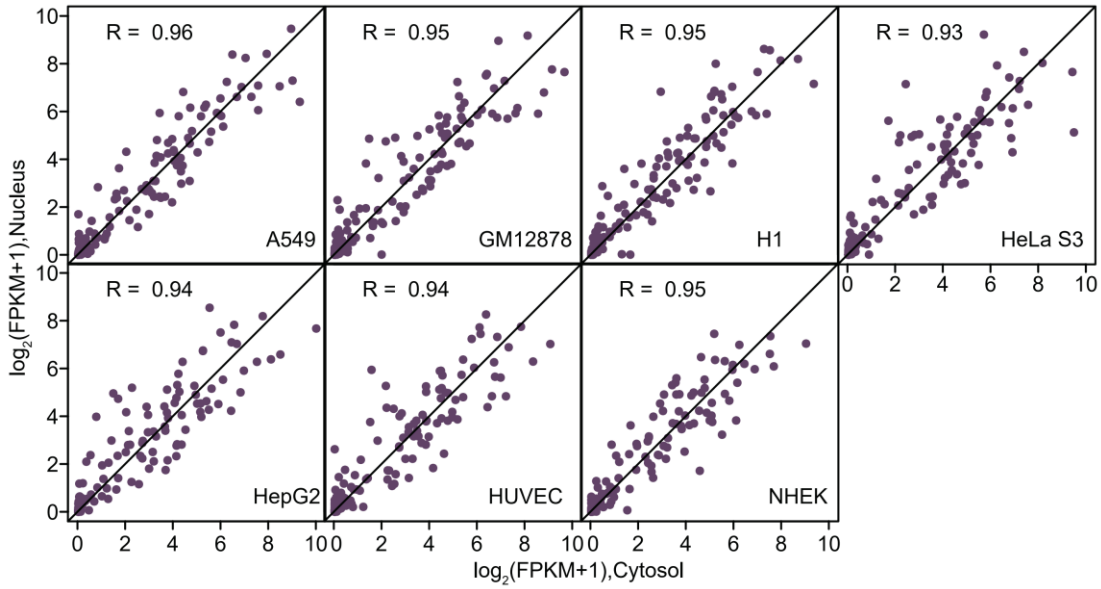

Supplemental Figure S6. Comparison of miRNA-AT expression levels between nuclear and cytosolic fractions of the cells.

Stranded mRNA-seq data of nuclear and cytoplasmic RNAs from 7 cell lines of the ENCODE Project were used for analysis.

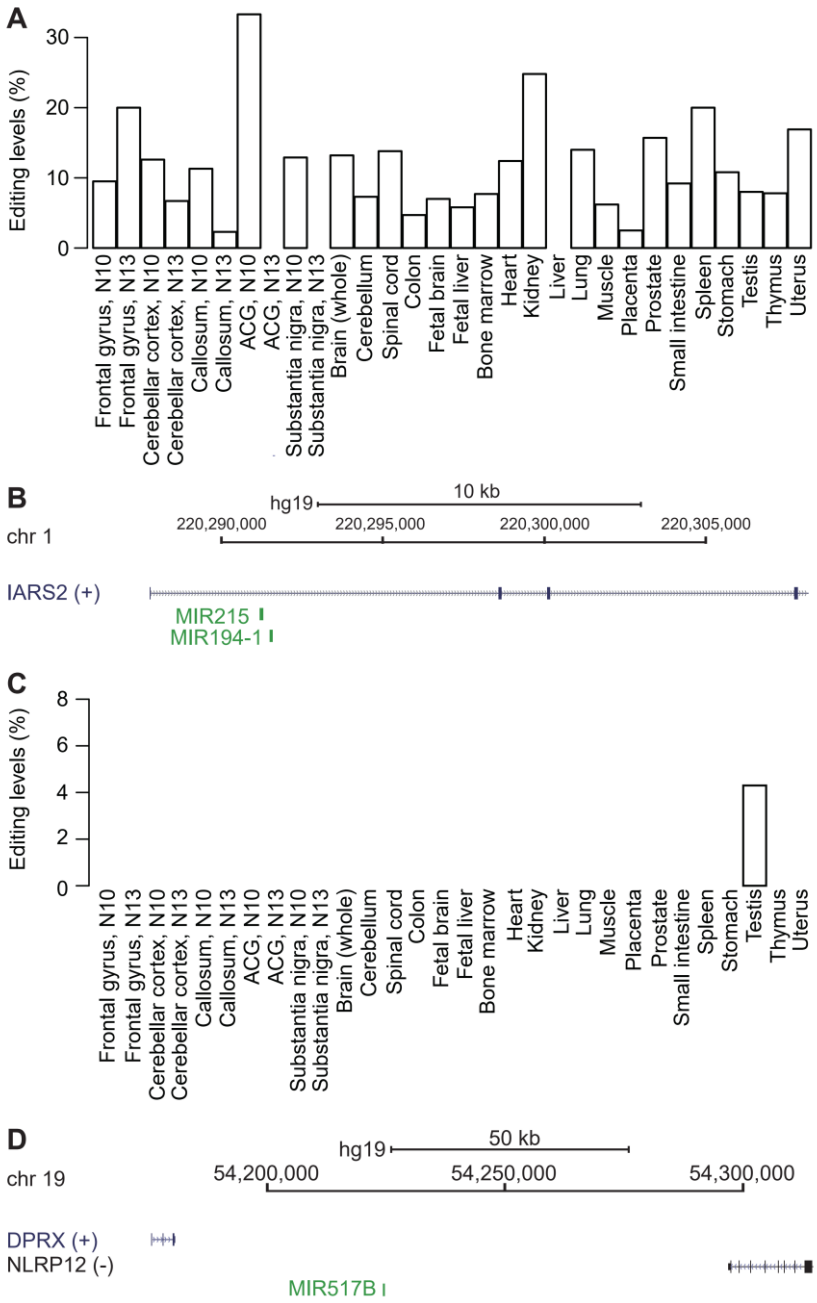

Supplemental Figure S7. Examples of miRNA-ATs.

(A) The editing level of miRNA-215-AT in the tissues we profiled. The site with the highest editing level in this miRNA-AT was shown.

(B) The UCSC Genome Browser shows that the region of miRNA-215-AT that is opposite to pre-miRNA-215 is in the intron of a protein-coding gene IARS2.

(C) The editing level of miRNA-517b-AT in the tissues we profiled. The site with the highest editing level in this miRNA-AT was shown.

(D) The UCSC Genome Browser shows that the region of miRNA-517b-AT that is opposite to pre-miRNA-517b is in the intergenic region.

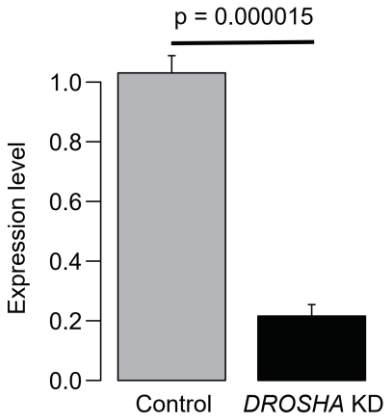

Supplemental Figure S8. *DROSHA* expression levels in control and knockdown cells.

Error bars, s.d. based on three biological replicates. P values were calculated using student's *t*-test.

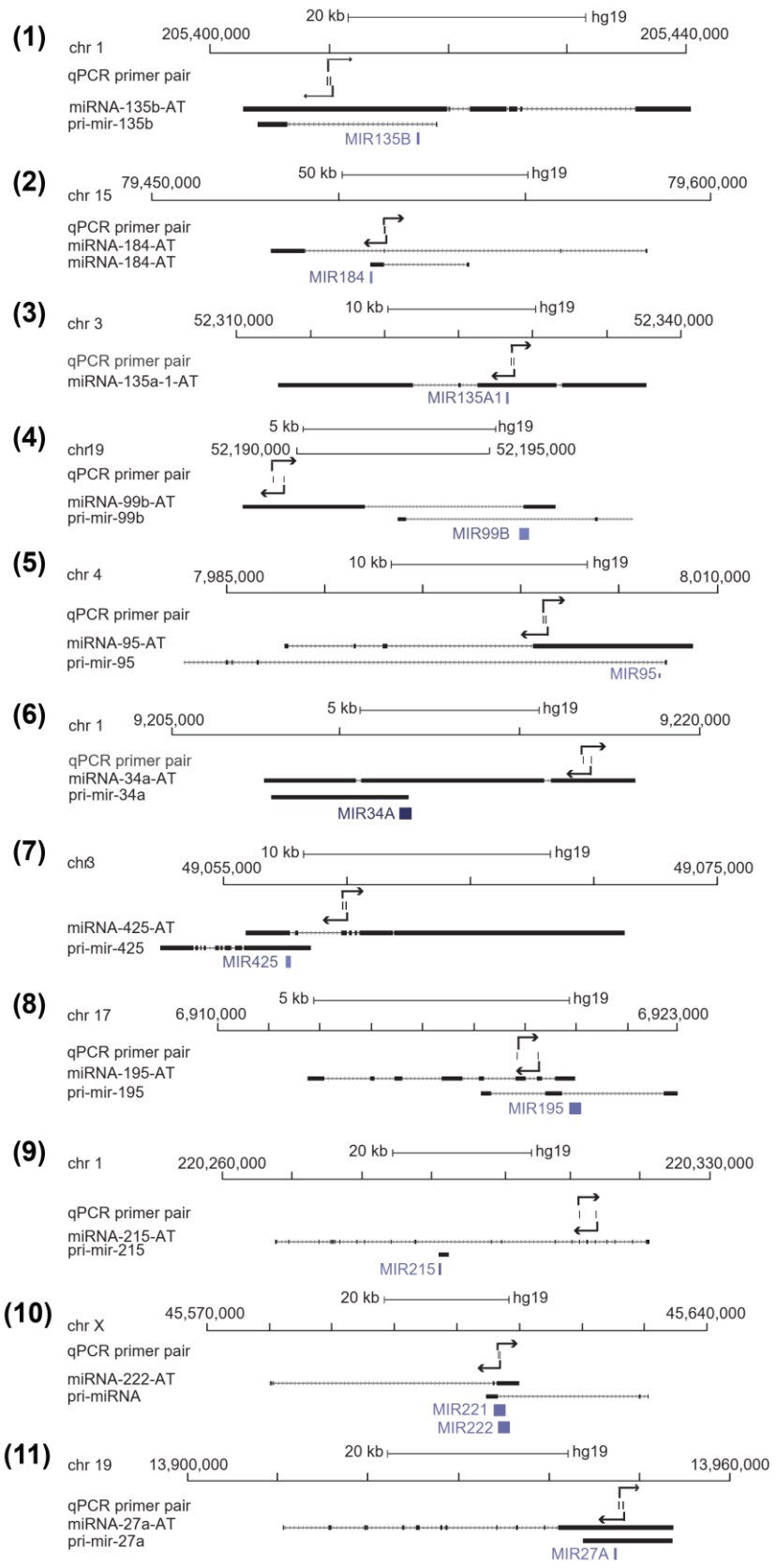

Supplemental Figure S9. The locations of primers used for miRNA-AT quantification upon *DROSHA* knockdown.

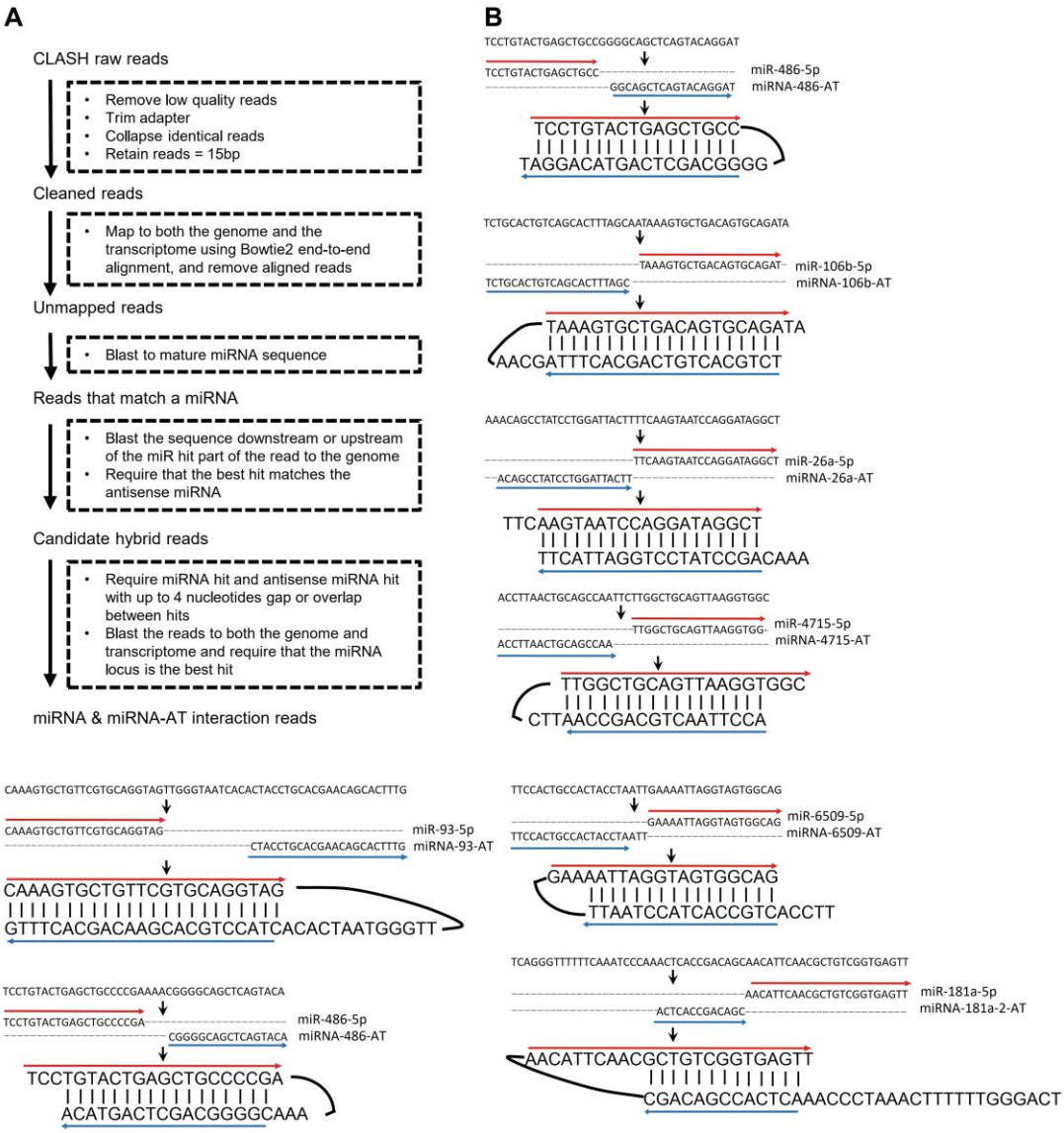

Supplemental Figure S10. CLASH data identified the interaction between miRNAs and miRNA-ATs.

(A) The Pipeline to deduce miRNA and miRNA-AT interaction using Ago-CLASH data.

(B) Details of putative interactions between mature miRNAs and their antisense transcripts identified from Ago-CLASH data.

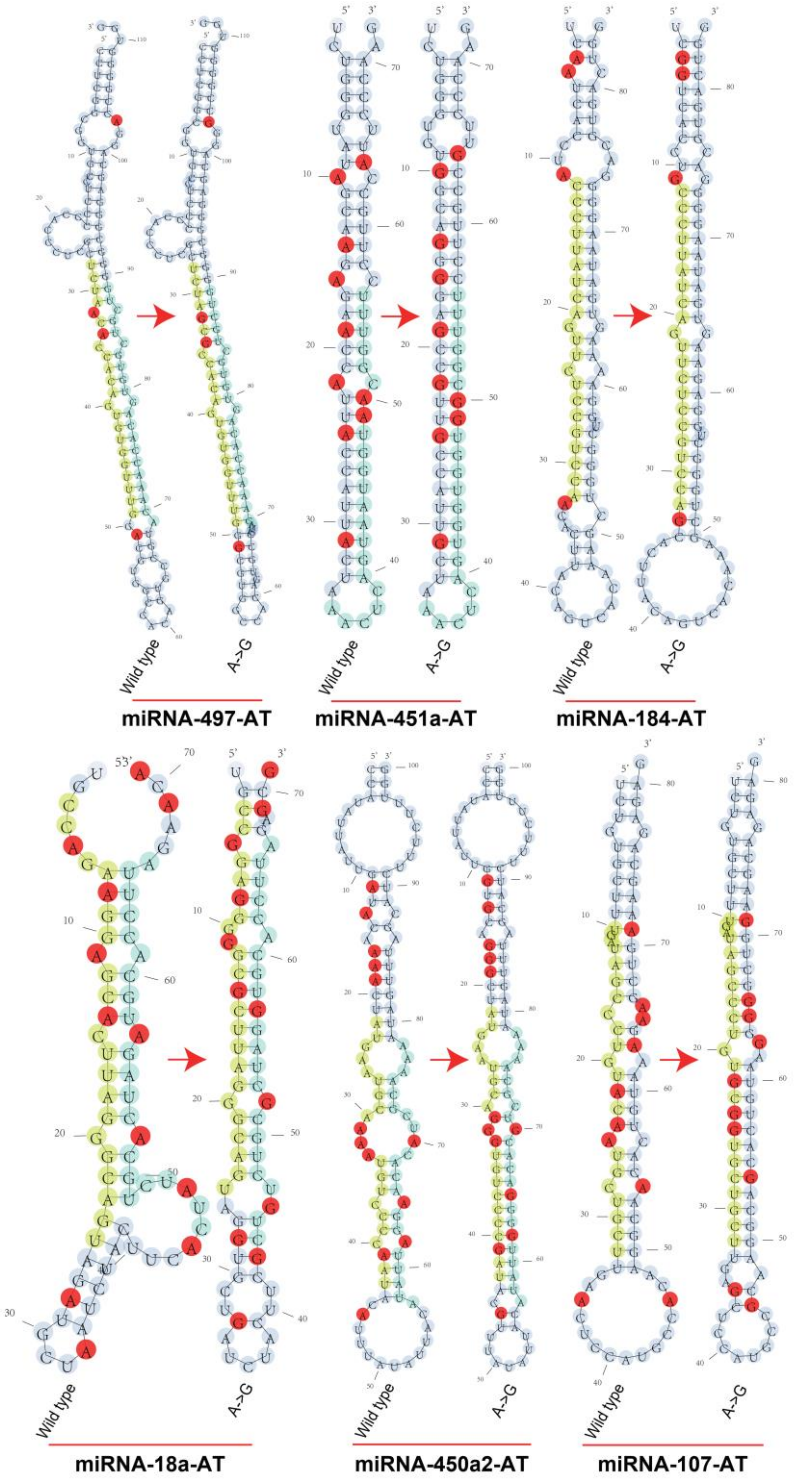

Supplemental Figure S11. RNA editing alters the secondary structure.

Predicted RNA secondary structure of unedited and edited forms of miRNA-ATs selected for reporter assay. The “A” or “G” nucleotide at the editing site is highlighted in red. Light blue and yellow sequences correspond to the regions opposite to the sense mature miRNA 5p and 3p, respectively.

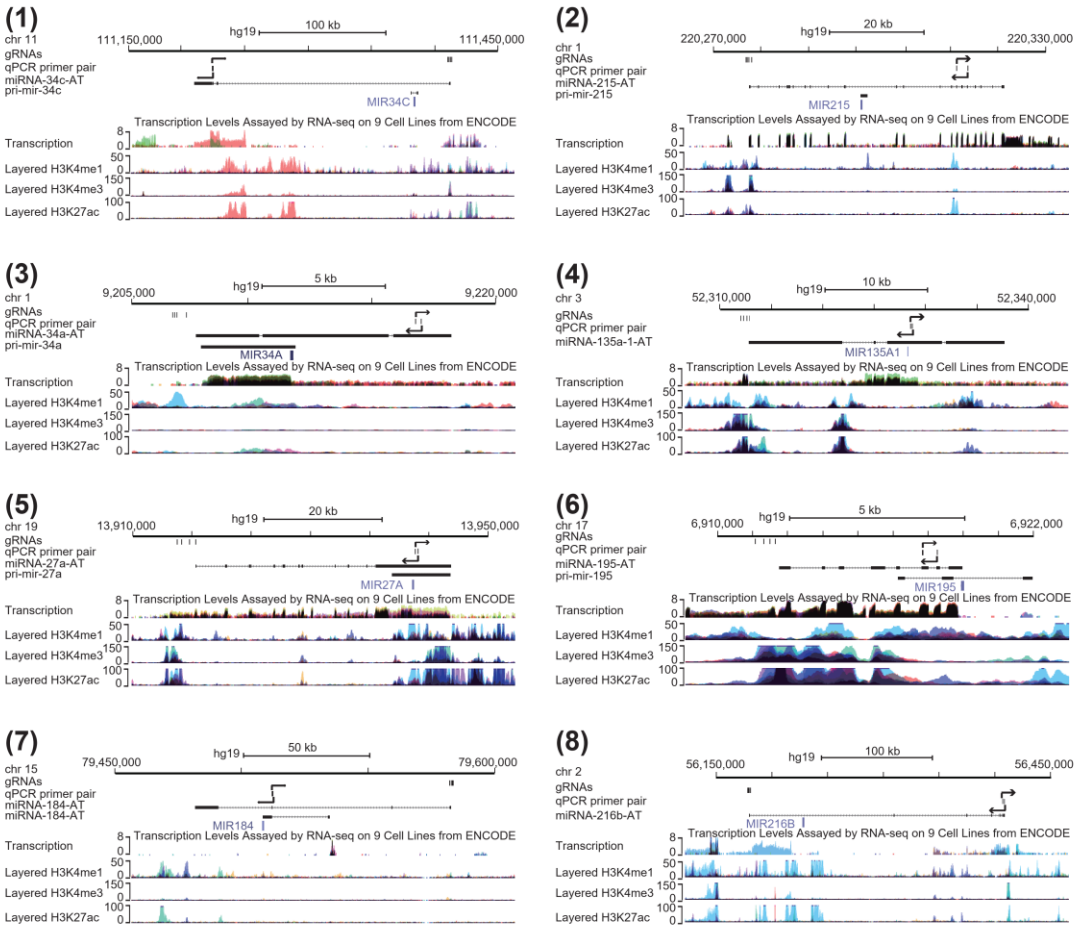

Supplemental Figure S12. Various genomic and chromatin features of sense-antisense miRNA pairs selected for CRISPRa experiments.

Various genomic and chromatin features of a sense-antisense miRNA pair were shown from top to bottom: 1) the positions of the 4 gRNAs used for miRNA-AT activation; 2) the location of the primer pair used to measure miRNA-AT expression; 3) the annotation of the full-length miRNA-AT from FANTOM5; 4) the annotation of the miRNA transcript from previous studies; 5) transcription levels assayed by RNA-seq on 9 Cell Lines from ENCODE; 6) three histone marks associated with regulatory elements and promoter from the ENCODE.

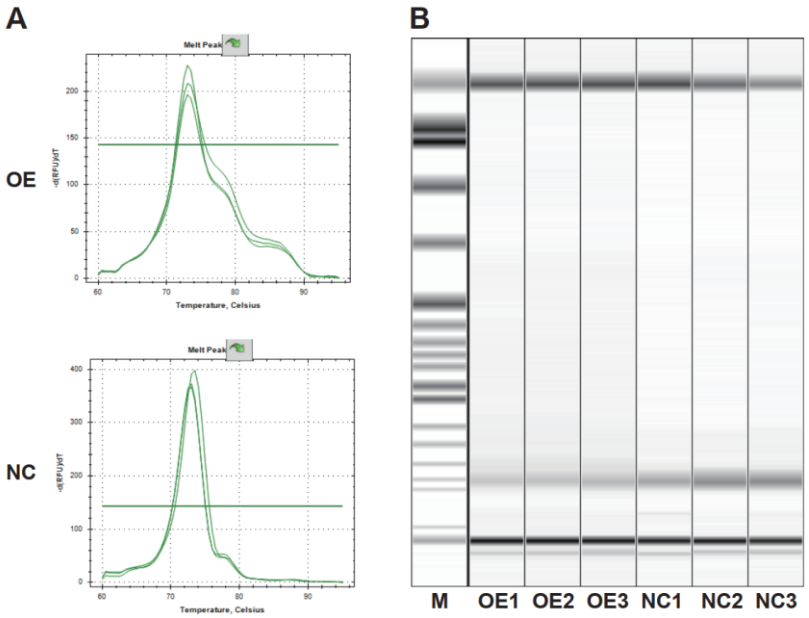

Supplemental Figure S13. Comparison of sense mature miR-135b-5p expression between miRNA-135b-AT overexpressed cells and control cells.

(A) Melting curve analysis of the real-time PCR assay. We found that the cells with miRNA-135b-AT overexpressed showed multiple peaks, which is likely due to the low expression level of miR-135b-5p. We therefore chose to use gel electrophoresis to quantify the expression of miR-135b-5p instead.

(B) Gel electrophoresis of the real-time PCR products using Qsep1 Portable DNA Analyzer. The red arrow indicates the PCR products. M, marker; OE, cells with miRNA-135b-AT overexpressed; NC, control cells. Three biological replicates were analyzed.

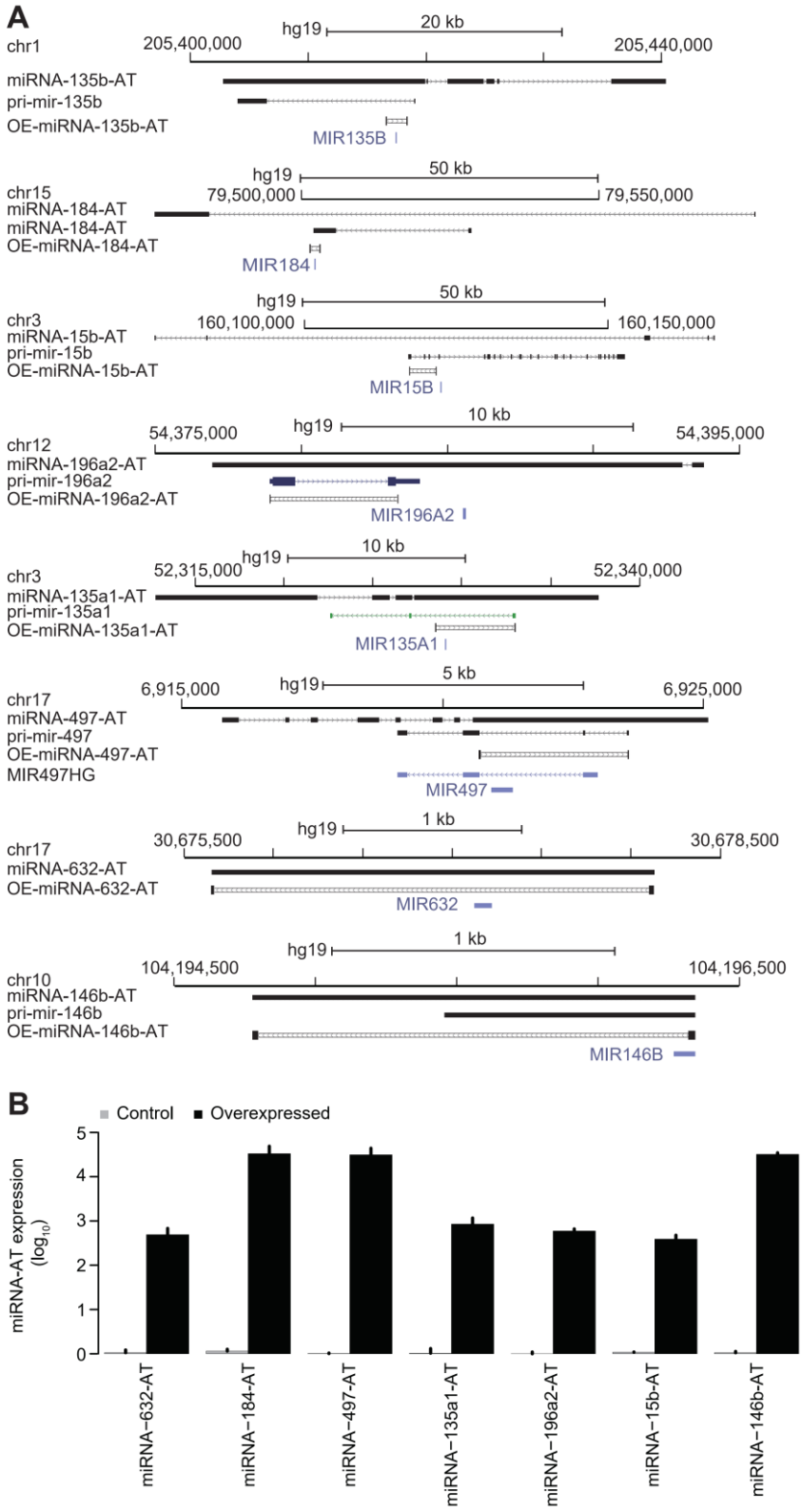

Supplemental Figure S14. Sense-antisense miRNA pairs selected for miRNA-AT overexpression experiments.

(A) Annotations of sense-antisense miRNA pairs were shown from top to bottom: 1) the full-length miRNA-AT from FANTOM5; 2) the pri-miRNA transcript from

previous studies; 3) the miRNA-AT fragment cloned for overexpression; 4) sense mature miRNA.

(B) RNA expression of miRNA-ATs in HEK293T cells transfected with expression vectors harboring individual miRNA-ATs. Control cells were transfected with the empty expression vectors. Error bars, s.d. based on three biological replicates.

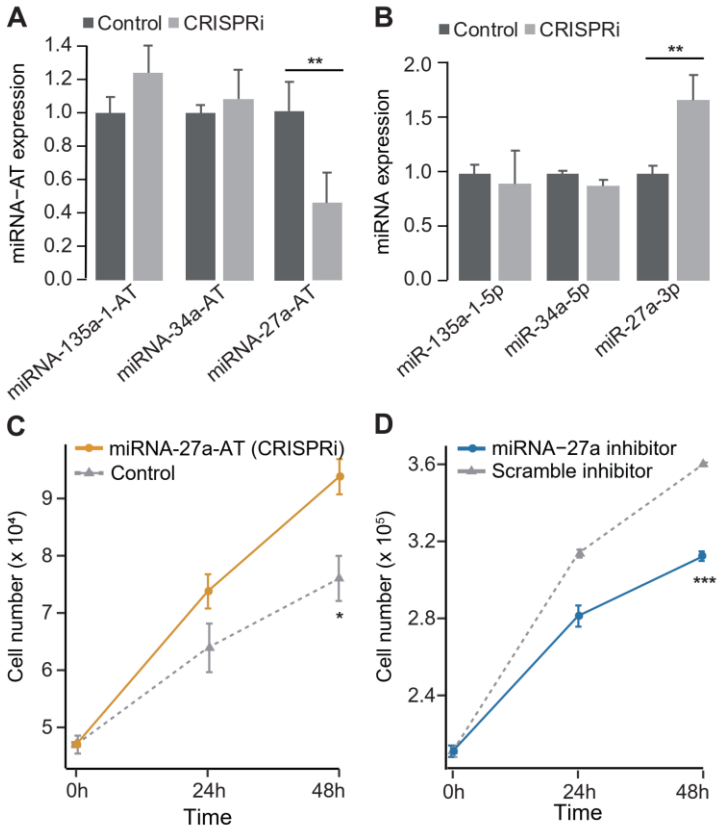

Supplemental Figure S15. miRNA-27a-AT negatively regulates miR-27a expression and affects cell proliferation.

(A) RNA expression of miRNA-ATs in HEK293T cells transfected simultaneously with four gRNAs targeting the indicated miRNA-ATs along with the dCas9-repressor construct. Control cells were transfected with the indicated guide RNAs alone. Error bars, s.d. based on three biological replicates. P values were calculated using student's *t*-test.

(**B**) RNA expression of mature miR-27a in HEK293T cells transfected simultaneously with four gRNAs targeting miRNA-27a-AT along with the dCas9-repressor construct. Control cells were transfected with the indicated guide RNAs alone. Error bars, s.d. based on three biological replicates. P values were calculated using Student's *t*-test.

(**C-D**) Comparison of the number of cells in different time points between control cells and cells with decreased transcription of miRNA-27a-AT (**C**) or between cells transfected with a scramble inhibitor and cells transfected with miR-27a inhibitor (**D**). Data are presented as Mean ± SEM (n = 4). The p values were determined using Student's *t*-test. *, $p<0.05$; ***, $p<0.001$.

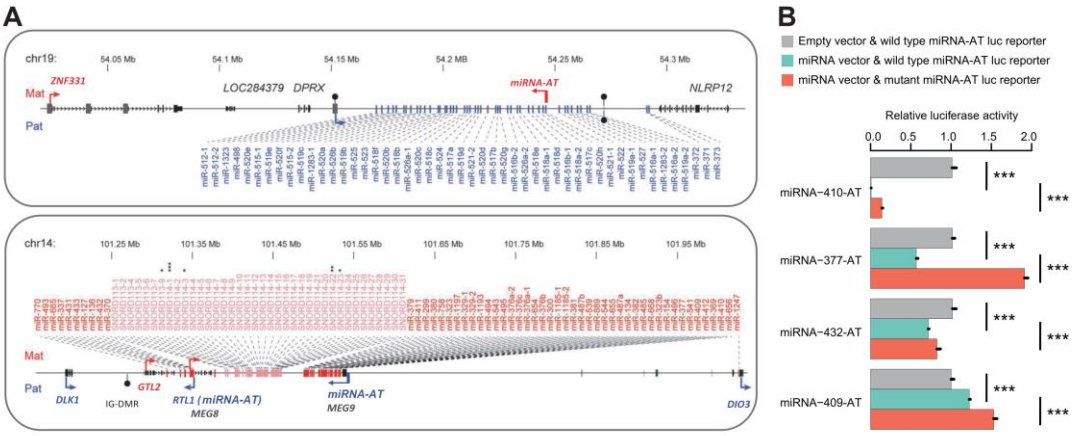

Supplemental Figure S16. Examples of miRNA-ATs in imprinted loci.

(A) The locations of miRNA-ATs in two known imprinted loci. The diagram of imprinted loci is adapted from Michael Girardot et al (Epigenetics. 2012).

(B) Dual-luciferase reporter assays to detect the effect of sense miRNAs on miRNA-AT expression. The experiments were performed as described in **Fig. 3B**. Four miRNA-ATs from the chr14 imprinted locus were randomly selected and 3 out of 4 were downregulated by the sense miRNAs.